Ammonia-assisted vapour transport deposition of formamidinium salts for perovskite thin films

Florent Sahli,*[a] Quentin Guesnay,[a] Niccolò Salsi, [a] Léo Duchêne,[b] Christophe Ballif,[a,c] Quentin Jeangros[a]

[a.] *Ecole Polytechnique Fédérale de Lausanne (EPFL), Institute of Microengineering (IMT), Photovoltaics and Thin-Film Electronics Laboratory, Rue de la Maladière 71b, 2002 Neuchâtel, Switzerland.*

[b.] *Empa, Swiss Federal Laboratories for Materials Science and Technology, Laboratory Materials for Energy Conversion, 8600 Dübendorf, Switzerland.*

[c.] *CSEM, PV-Center, Jaquet-Droz 1, 2002 Neuchâtel, Switzerland.*

Abstract

Formamidinium (FA) cations commonly used in perovskite semiconductors tend to form sym-triazine when sublimed in vacuum, a process that hampers the deposition process. Here we find that ammonia, when used as a carrier gas for formamidinium halides transport, cleaves the sym-triazine ring back to formamidinium, hence enhancing the deposition efficiency.

Organic-inorganic metal-halide perovskite solar cells are promising building blocks of the next generation of photovoltaic technologies due to their high power conversion efficiency and potential for low manufacturing costs.[1] While most studies reported to date have employed solution processing, vapour-based processes are promising alternatives to produce thin films on large, possibly textured, substrates with a high yield in a controlled environment.[2,3] Various perovskite vapour-based techniques have been reported, notably physical vapour deposition (PVD), where both inorganic and organic precursors are sublimed in a high-vacuum chamber (typically 10^{-5} to 10^{-6} mbar), either simultaneously (1-step) or subsequently (2-step process).[4,5] While these methods produce perovskite thin films that yield solar cell efficiencies over 20%,[6] precisely controlling the sublimation/deposition rate of the organic cations is still a complex task.[7] This issue is mainly related to their high vapour pressure, which leads to their deposition everywhere in the chamber and favours their desorption from chamber walls and from the quartz crystal monitor(s) supposed to measure the deposition rate. Alternatively, chemical vapour deposition (CVD) in low vacuum condition (mbar range) and hybrid PVD-CVD methods have been demonstrated.[8,9] The use of a carrier gas in CVD processes to transport the sublimed species to heated substrates provides additional process control as the flow rate can be tuned.[10,11]

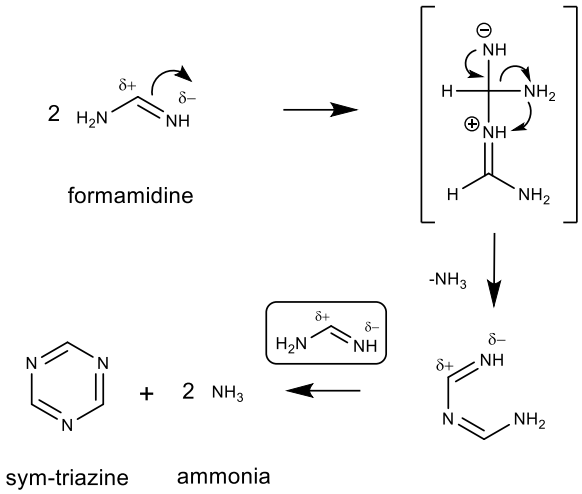

Figure 1: Detailed chemical mechanism of the condensation reaction of formamidine to sym-triazine. δ indicates partial charge on the molecule.

While various strategies have been setup to improve process control of PVD and/or CVD methods, depositing organohalides from their vapours presents some intrinsic challenges. It was recently reported that formamidinium iodide, the key organic component of most high-efficiency solar cells, reacts to form a volatile compound, sym-triazine, when heated on its own or as part of a fully formed perovskite layer through a condensation reaction (**Figure 1**).[12] The reaction is triggered by the nucleophilic attack of the carbon by the amine groups of the FA molecule, leading to a linear dimer and releasing ammonia as by-product. A third FA molecule closes the heterocycle ring (**Figure 1**). It was reported that sym-triazine can also be produced with a high-yield when condensing FACl molecules in a basic solution or in the vapour phase.[13,14] Increasing the temperature and reducing pressure push the reaction in favour of sym-triazine and ammonia production. It hence appears likely that sym-triazine may form upon FA salts sublimation, overall impeding the perovskite deposition process.

We first confirm that sym-triazine can indeed form upon heating/sublimating FA salts in atmospheric conditions. A thermogravimetry coupled with mass spectrometry (TGA-MS) analysis of FAI from 160 °C to 240 °C (temperatures typically used to evaporate FAI) reveals that, while FA+ (m/z= 42-44) can be observed at 240 °C, sym-triazine and its fragment (m/z= 81, 80 and 54) are by far the most significant by-products of the evaporation at each temperature tested (**Figure 2** and Figure S1). Note that the reduction in both signals at 240 °C comes from the fact that most of the precursor has been already consumed. Sym-triazine has a low melting point of 81-86 °C and its vapours are stable up to 600 °C before they degrade into hydrogen cyanide.[14] As the temperatures used to evaporate FAI to produce perovskite thin films usually do not exceed 200 °C, sym-triazine is expected to form and remain present.

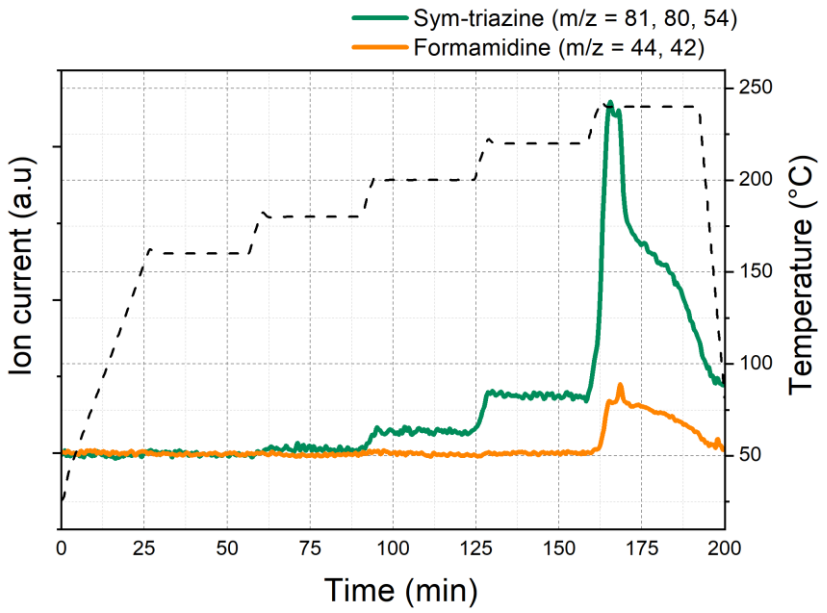

Figure 2: TGA-MS isotherms of FAI. the contribution from formamidine ions (m/z = 42 and 44) are represented by the orange line, whereas sym-triazine molecules (m/z = 81, 80) and its fragment (HCN–(H)CN, m/z = 54) are represented by the green line. The dashed line represents the temperature profile of the TGA-MS experiment.

In view of producing perovskite thin films, we then assess whether sym-triazine vapours can react with PbI_2 to form a perovskite layer. To do so, we employ a home-built vapour transport deposition (VTD) system for perovskite deposition over large areas (239 cm^2, the dimension of a 6 inch M2 Si wafer). The system consists in a temperature-controlled evaporation unit where the precursor is placed in a crucible. A carrier gas is used to bring the sublimed vapours through a showerhead and into the deposition chamber. The carrier gas, chamber walls and showerhead are heated to prevent any condensation of the precursor before reaching the lead halide templates, which are placed on a temperature-controlled deposition table (adjustable from 80 to 160 °C). The exhaust of the chamber is placed directly below the deposition table and is connected to a primary pump. More information about the VTD setup can be found elsewhere.[15] Sym-triazine was evaporated in this system, while keeping the substrates coated with a thermally evaporated layer of 150 nm of PbI_2/CsBr (atomic ratio of Cs/Pb of ~0.2) at low temperature ($T_{substrate}$ = 80 °C) to condense the organic molecules. From the liquid ^{1}H nuclear magnetic resonance (NMR) analysis of the condensate (collected on PbI_2/CsBr and dissolved in DMSO-d6), we were not able to detect any sym-triazine when N_2 was used as a carrier gas, as evidenced by the absence of the ^{1}H proton peak at 9.3 ppm (**Figure 3a**). It appears that sym-triazine neither sticks nor reacts with the evaporated PbI_2/CsBr templates, preventing any perovskite formation. The latter point is confirmed when spin-coating sym-triazine (dissolved in IPA) directly on PbI_2/CsBr templates (Figure S2).

Primary amines such as ammonia have been shown to cleave the heterocycle ring of sym-triazine through a nucleophilic attack of the carbon on the aromatic ring.[16,17] To assess whether the reaction depicted **Figure 3b** can indeed be triggered in our VTD system, sym-triazine was sublimed in the reactor and, this time, transported by NH_3 to the deposition chamber instead of N_2. The deposition table was maintained at the same low temperature ($T_{substrate}$ = 80 °C) to enable the condensation of organic molecules on the PbI_2/CsBr substrates. As shown in **Figure 3a,** formamidinium cations are this time detected on the substrate, as highlighted by the ^{1}H resonance from the 2 amine groups at 8.65 and 9 ppm.[18] The peaks observed at 7.85 ppm correspond to the proton on the carbon atom. NH_3 is hence able to cleave sym-triazine, resulting in the deposition of

formamidinium cations. While such a pathway could potentially be used to form perovskite layers, sym-triazine was found to be highly volatile, leaving little time for it to react with NH_3.

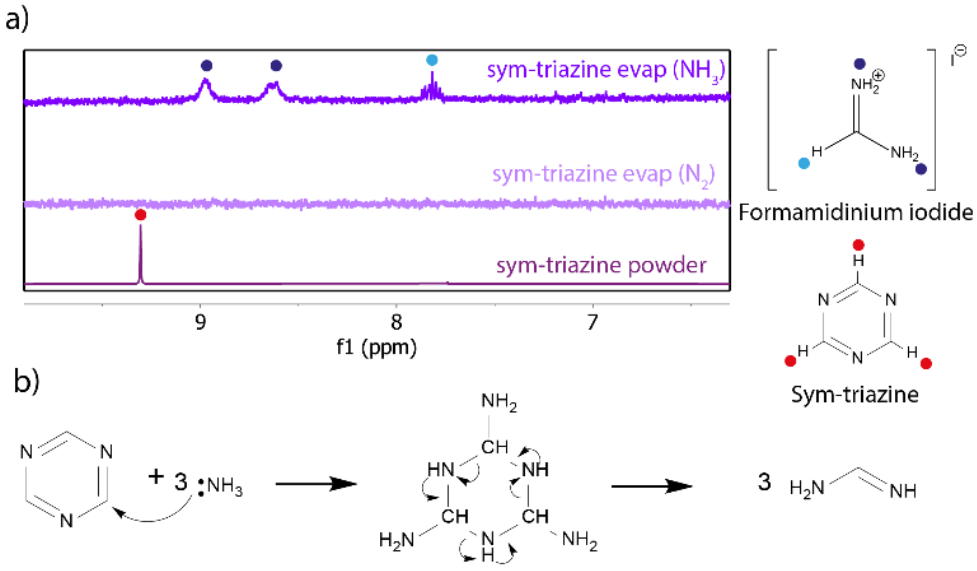

Figure 3: a) Liquid ^{1}H NMR of the sym-triazine powder and sym-triazine evaporated using either N_2 or NH_3 as carrier gas. b) Chemical degradation reaction triggered by the nucleophilic attack of ammonia on sym-triazine, which results in the formation of formamidine.

To increase the residence time and the probability of cleaving sym-triazine with NH_3, a PbI_2/CsBr coated substrate and recipients containing sym-triazine, ammonia and I_2 were sealed in a glass box, which was placed on a hotplate and heated to 160 °C for 60 min (Figure S3a-b). I_2 acts as a halide source, which favours the formation of the perovskite. **Figures 4a** displays X-ray diffractograms of the PbI_2/CsBr templates before and after the deposition process. A photoactive perovskite phase forms in these conditions, even though a significant amount of PbI_2 remain and oversaturated hydrated phases form upon air exposure.[15] Liquid ^{1}H NMR measurement of the dissolved film after deposition confirms the presence of formamidinium cations within the layer (**Figure 4b**). This observation validates that sym-triazine can indeed be cleaved by ammonia to yield FA cations. Similar conclusions were obtained without the presence of the halide source (Figure S3c). The presence of a halide source on its own can also lead to the cleavage of the sym-triazine heterocycle (Figure S3c).

Now that we have seen that sym-triazine can be cleaved into formamidine in the presence of NH_3, FAI was evaporated in our VTD setup using either N_2 or NH_3 as carrier gas. The evaporation parameters were set to $T_{crucible}$ = 210 °C, $T_{substrate}$ = 140 °C, and the working pressure to 8.85 mbar by setting the appropriate amount of carrier gas. During the deposition process, the temperature of the table was maintained at 140 °C to directly convert the PbI_2/CsBr templates to a perovskite (CVD growth regime). The evaporation was performed for 4 hours with samples being analysed after each hour of evaporation. First, FAI was evaporated using N_2 as a carrier gas. **Figure 5a** shows X-ray diffractograms of the PbI_2/CsBr layer before and after evaporating FAI in the VTD system for 1 to 4 hours. With these evaporation parameters, the CsBr/PbI_2 templates did not react with FAI, as evidenced by the absence of perovskite diffraction peaks (**Figure 5a**). Perovskite phase traces eventually forms after 8 hours of evaporation (Figure S4). These results indicate that the conversion to the perovskite phase is still happening but at an extremely slow rate. It is worth mentioning that numerous studies have reported the successful deposition of FA salts in high-vacuum PVD chamber or lower-vacuum tube furnaces.[10,19] The difference between these reports and our observations stems from the larger distance that the sublimed vapours have to travel in our setup from the

evaporation unit to the deposition table (>100 cm compared to typically ≈ 20 cm usually). When we place the PbI_2/CsBr substrate to convert close to the evaporation unit of our VTD chamber, a full perovskite conversion occurs within 1 hour (Figure S5). In short, the sym-triazine formation reaction described in **Figure 1** occurs during the vapour transport process, an aspect that will have to be taken into account if/when up-scaling VTD towards industry-relevant dimensions.

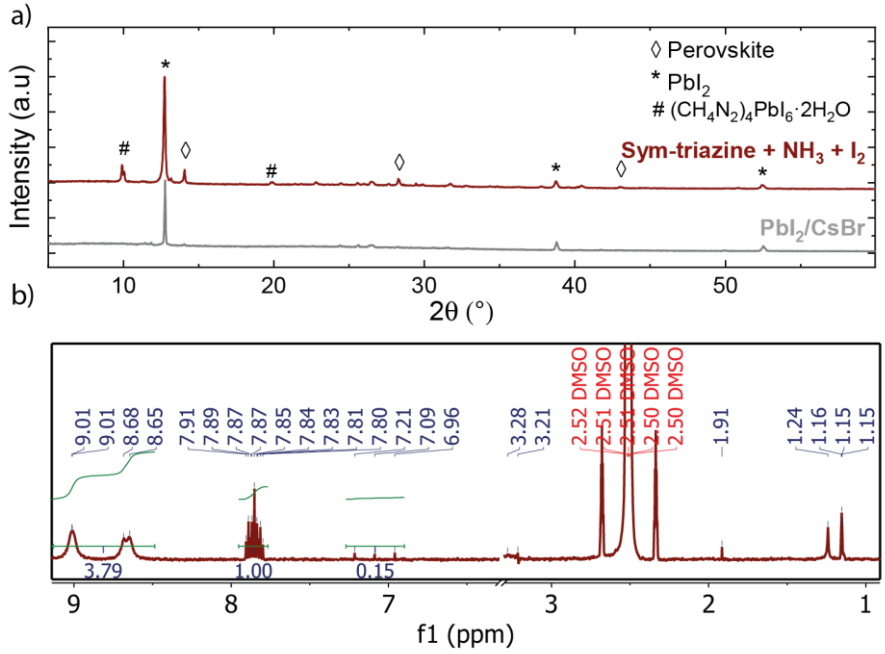

Figure 4: a) X-ray diffractograms of the initial PbI_2/CsBr film after 10 min of sym-triazine evaporation with NH_3 and I_2 and b) corresponding liquid ^{1}H NMR of PbI_2/CsBr film dissolved in DMSO-d6.

Figure 5b displays pictures of PbI_2/CsBr layers exposed between 1 to 4 hours to organohalide vapours carried to the substrates using NH_3. When using NH_3 instead of N_2, a perovskite is forming already after 1 hour (instead of 8 hours with N_2). X-ray diffractograms of the layers confirm that a full perovskite conversion is obtained after 3 hours of evaporation, a fraction of the time that is needed with N_2 (**Figure 5b**). In addition, liquid ^{1}H NMR measurement of the layer after 4 h of deposition shows the characteristic peaks of the FA cation (Figure S6) with only a few NH_4I impurities (NH_4I:FAI ratio of 1:15 for NH_3 compared to 233:1 when N_2 is used, values obtained from peaks integration of ^{1}H NMR data). These experiments demonstrate that the use of NH_3 as carrier gas for FAI significantly improves the deposition efficiency, which may prove critical when up-scaling deposition chambers to deposit perovskite semiconductors over large areas. The use of ammonia as a carrier gas also enables the deposition of other formamidinium salts, namely FABr, FACl and FAAc, a feat that we could not achieve when using N_2 (Figure S7).

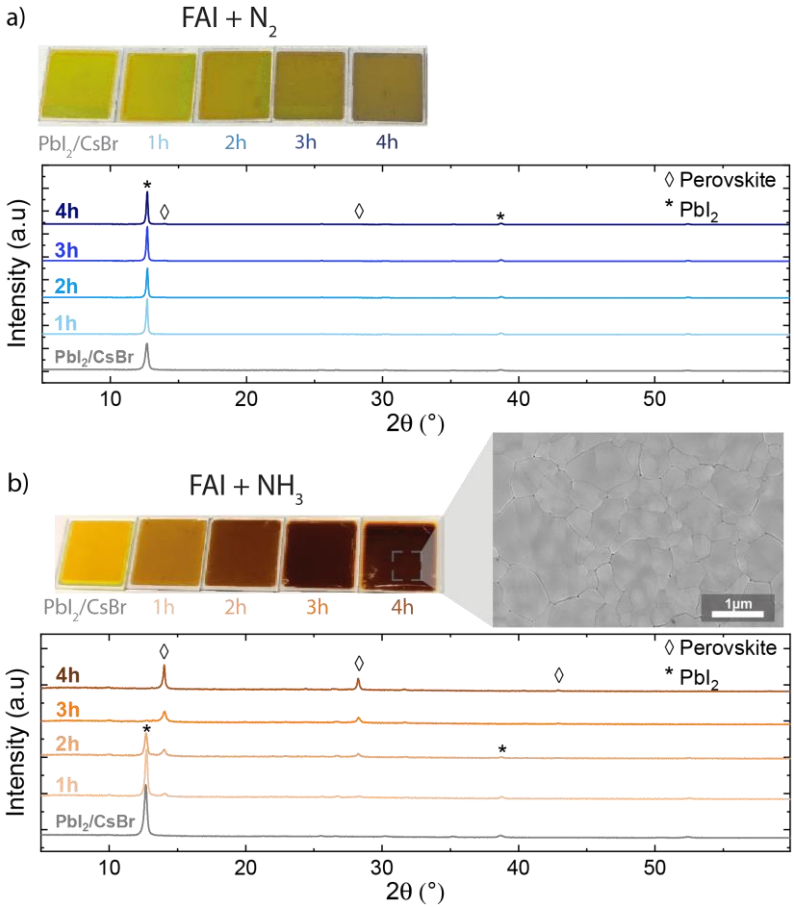

Figure 5: a) X-ray diffractograms and pictures of PbI_2/CsBr layers before and after FAI evaporation with N_2 as carrier gas ($T_{substrate}$ = 140 °C, 1 to 4 hours of evaporation), b) corresponding experiment when NH_3 is used as a carrier gas. The inset is a top view scanning electron microscopy image of the perovskite layer.

In conclusion, once sublimed, the formamidinium cations typically employed in high-efficiency perovskite solar cells tend to form sym-triazine in the vapour phase. This reaction has several implications when depositing these materials by PVD/CVD: it increases the material usage and significantly slows down the production of perovskite thin films, especially when using large reactors where the sublimed vapours take some time to reach the substrates to coat. We show here that using NH_3 as a carrier gas instead of N_2 to bring the sym-triazine-rich vapours of FA salts can reverse the reaction and cleave sym-triazine back to formamidine. We demonstrate the effectiveness of this NH_3-based approach by converting PbI_2/CsBr templates to a perovskite phase at a significantly accelerated conversion efficiency compared to N_2. This approach may be relevant at the industrial level in view of producing perovskite thin films over large areas using vapour transport deposition. In addition, sym-triazine may also be used directly as a precursor with NH_3 to form perovskite layers. This alternative appears promising as sym-triazine has a higher vapour pressure than FAI, which should lead to faster deposition processes. Finally, other heterocyclic molecules such as melamine or melamine iodide salts may be potentially used as organic precursors with this method.

The authors would like to acknowledge financial supports from the Swiss Federal Office of Energy (SI/501804-01 INTENT) and the Swiss National Science Foundation (176552 Bridge Power, CRSII5 171000 Sinergia Episode project.

Conflicts of interest

There are no conflicts to declare

Notes and references

(1) Green, M. A.; Ho-Baillie, A.; Snaith, H. J. The Emergence of Perovskite Solar Cells. *Nat. Photonics* **2014**, *8*, 506. https://doi.org/10.1038/NPHOTON.2014.134.

(2) Qiu, L.; He, S.; Jiang, Y.; Son, D. Y.; Ono, L. K.; Liu, Z.; Kim, T.; Bouloumis, T.; Kazaoui, S.; Qi, Y. Hybrid Chemical Vapor Deposition Enables Scalable and Stable Cs-FA Mixed Cation Perovskite Solar Modules with a Designated Area of 91.8 Cm2 Approaching 10% Efficiency. *J. Mater. Chem. A* **2019**, *7* (12), 6920–6929. https://doi.org/10.1039/c9ta00239a.

(3) Borchert, J.; Milot, R. L.; Patel, J. B.; Davies, C. L.; Wright, A. D.; Martínez Maestro, L.; Snaith, H. J.; Herz, L. M.; Johnston, M. B. Large-Area, Highly Uniform Evaporated Formamidinium Lead Triiodide Thin Films for Solar Cells. *ACS Energy Lett.* **2017**, *2* (12), 2799–2804. https://doi.org/10.1021/acsenergylett.7b00967.

(4) Liu, M.; Johnston, M. B.; Snaith, H. J. Efficient Planar Heterojunction Perovskite Solar Cells by Vapour Deposition. *Nature* **2013**, *501* (7467), 395–398. https://doi.org/10.1038/nature12509.

(5) Chen, C.-W.; Kang, H.-W.; Hsiao, S.-Y.; Yang, P.-F.; Chiang, K.-M.; Lin, H.-W. Efficient and Uniform Planar-Type Perovskite Solar Cells by Simple Sequential Vacuum Deposition. *Adv. Mater.* **2014**, *26* (38), 6647–6652. https://doi.org/10.1002/adma.201402461.

(6) Zhu, X.; Yang, D.; Yang, R.; Yang, B.; Yang, Z.; Ren, X.; Zhang, J.; Niu, J.; Feng, J.; Liu, S. (Frank) F. Superior Stability for Perovskite Solar Cells with 20% Efficiency Using Vacuum Co-Evaporation. *Nanoscale* **2017**, *9* (34), 12316–12323. https://doi.org/10.1039/C7NR04501H.

(7) Borchert, J.; Levchuk, I.; Snoek, L. C.; Rothmann, M. U.; Haver, R.; Snaith, H. J.; Brabec, C. J.; Herz, L. M.; Johnston, M. B. Impurity Tracking Enables Enhanced Control and Reproducibility of Hybrid Perovskite Vapour Deposition. *ACS Appl. Mater. Interfaces* **2019**, acsami.9b07619. https://doi.org/10.1021/acsami.9b07619.

(8) Chen, Q.; Zhou, H.; Hong, Z.; Luo, S.; Duan, H. S.; Wang, H. H.; Liu, Y.; Li, G.; Yang, Y. Planar Heterojunction Perovskite Solar Cells via Vapor-Assisted Solution Process. *J. Am. Chem. Soc.* **2014**, *136* (2), 622–625. https://doi.org/10.1021/ja411509g.

(9) Hoerantner, M. T.; Wassweiler, E. L.; Zhang, H.; Panda, A.; Nasilowski, M.; Osherov, A.; Swartwout, R.; Driscoll, A. E.; Moody, N. S.; Bawendi, M. G.; Jensen, K. F.; Bulović, V. High-Speed Vapor Transport Deposition of Perovskite Thin Films. *ACS Appl. Mater. Interfaces* **2019**, *11* (36), 32928–32936. https://doi.org/10.1021/acsami.9b07651.

(10) Qiu, L.; He, S.; Jiang, Y.; Son, D.-Y.; Ono, L. K.; Liu, Z.; Kim, T.; Bouloumis, T.; KAZAOUI, S.; Qi, Y. Hybrid Chemical Vapor Deposition Enables Scalable and Stable Cs-FA Mixed Cation Perovskite Solar Modules with a Designated Area of 91.8 Cm2 Approaching 10% Efficiency. *J. Mater. Chem. A* **2019**. https://doi.org/10.1039/C9TA00239A.

(11) Leyden, M.; Ono, L.; Raga, S.; Kato, Y.; Wang, S.; Qi, Y. High Performance Perovskite Solar Cells by Hybrid Chemical Vapor Deposition. *J. Mater. Chem. A* **2014**, *2* (44), 18742–18745. https://doi.org/10.1039/c4ta04385e.

(12) Juarez-Perez, E. J.; Ono, L. K.; Qi, Y. Thermal Degradation of Formamidinium Based Lead Halide Perovskites into: Sym -Triazine and Hydrogen Cyanide Observed by Coupled Thermogravimetry-Mass Spectrometry Analysis. *J. Mater. Chem. A* **2019**, *7* (28), 16912–16919. https://doi.org/10.1039/c9ta06058h.

(13) Schaefer, F. C.; Hechenbleikner, I.; Peters, G. A.; Wystrach, V. P. Synthesis of the Sym-Triazine System. I. Trimerization and Cotrimerization of Amidines. *J. Am. Chem. Soc.* **1959**, *81* (6), 1466–1470. https://doi.org/10.1021/ja01515a046.

(14) Grundmann, C. New Methods in Preparative Organic Chemistry Syntheses with S-Triazine. *Angew. Chemie - Int. Ed.* **1963**, *2* (6), 309.

(15) Sahli, F.; Miaz, N.; Salsi, N.; Bucher, C.; Schafflutzel, A.; Guesnay, Q.; Duchêne, L.; Niesen, B.; Ballif, C.; Jeangros, Q. Vapour Transport Deposition of Methylammonium Iodide for Perovskite Solar Cells. *ACS Appl. Energy Mater.* **2021**. https://doi.org/10.1021/acsaem.0c02999.

(16) Grundmann, C.; Kreutzberger, A. Triazines. XIII. The Ring Cleavage of s-Triazine by Primary Amines. A New Method for the Synthesis of Heterocycles. *J. Am. Chem. Soc.* **1956**, *77* (24), 6559–6562. https://doi.org/10.1021/ja01629a041.

(17) Grundmann, C.; Rätz, R. Triazines. XVI. A New Synthesis for 1,2,4-Triazoles. *J. Org. Chem.* **1956**, *21* (9), 1037–1038. https://doi.org/10.1021/jo01115a610.

(18) Van Gompel, W. T. M.; Herckens, R.; Reekmans, G.; Ruttens, B.; D'Haen, J.; Adriaensens, P.; Lutsen, L.; Vanderzande, D. Degradation of the Formamidinium Cation and the Quantification of the Formamidinium-Methylammonium Ratio in Lead Iodide Hybrid Perovskites by Nuclear Magnetic Resonance Spectroscopy. *J. Phys. Chem. C* **2018**, *122* (8), 4117–4124. https://doi.org/10.1021/acs.jpcc.7b09805.

(19) Gil-Escrig, L.; Momblona, C.; La-Placa, M. G.; Boix, P. P.; Sessolo, M.; Bolink, H. J. Vacuum Deposited Triple-Cation Mixed-Halide Perovskite Solar Cells. *Adv. Energy Mater.* **2018**, *8* (14), 1–6. https://doi.org/10.1002/aenm.201703506.

Supplementary Information

Ammonia-assisted vapour transport deposition of formamidinium salts for perovskite thin films

Florent Sahli,*[a] Quentin Guesnay,[a] Niccolò Salsi,[a] Léo Duchêne,[b] Christophe Ballif,[a,c] Quentin Jeangros[a]

[a.] *Ecole Polytechnique Fédérale de Lausanne (EPFL), Institute of Microengineering (IMT), Photovoltaics and Thin-Film Electronics Laboratory, Rue de la Maladière 71b, 2002 Neuchâtel, Switzerland.*

[b.] *Empa, Swiss Federal Laboratories for Materials Science and Technology, Laboratory Materials for Energy Conversion, 8600 Dübendorf, Switzerland.*

[c.] *CSEM, PV-Center, Jaquet-Droz 1, 2002 Neuchâtel, Switzerland.*

Experimental section

Lead halide templates preparation

Glass/indium tin oxide (ITO) substrates (15 Ohm/sq, Kintec) were cleaned by an oxygen plasma treatment and followed by a UV-Ozone treatment for 15 min. Then, 150 nm of PbI_2 (>99.99%, Alfa Aesar) and CsBr (>99.99%, Abcr) was evaporated in a Lesker Mini SPECTROS evaporation system (base pressure of < 2 x 10^{-6} mbar, working pressure of < 5 x 10^{-6} mbar, evaporation rate of 1 Å/s for PbI_2 and 0.2 Å/s for CsBr).

Vapour transport deposition of FAI

A detail description of the VTD setup can be found elsewhere.[1] The PbI_2/CsBr layers were taken out of the glovebox in air and placed on the VTD system deposition table at a temperature of 80 °C to condense the organics vapours (Figures 3 and S7) or at 140 °C to form the perovskite layer with FAI as the precursor (Figures 5, S4 and S6, CVD growth conditions). Approximately 1 g of fresh organic material (FAI, FACl, FABr, FAAc, sym-triazine) was placed in a graphite crucible. FAI (>99.99%), FACl (>99.99%), FABr (>99.99%) were purchased from Greatcell solar, FACl (>98%) was supplied by TCI and sym-triazine (>97%) by Sigma-Aldrich. The whole system (evaporator and deposition chamber) was then pumped down to a base pressure of 0.15 mbar (5 min of pumping). The carrier gas, either N_2 (>99.99%), or NH_3 (>99.98%), was then introduced by a Mass flow controller (MFC). Overall, the working pressure of the system was maintained at 8.85 mbar to ensure the same supply of both carrier gases (butterfly valve leading to the pump in closed position). The temperature of the crucible was increased to the desired temperature at a rate of ~10 °C/min, corresponding to 15 min to reach 210 °C. The evaporation was performed in steady-state conditions for 1 to 8 hrs. Once the evaporation finished, the temperature control of the evaporator was switched off and the substrates were removed from the deposition chamber.

Evaporation of sym-triazine in a sealed environment

The PbI_2/CsBr substrates were tapped to the lid of a glass container. The precursors, sym-triazine (>97%, Sigma-Aldrich, 45 mg), I_2 (>99.99%, Sigma Aldrich, 225 mg), NH_3 (30% in ethanol, Sigma Aldrich, 100 µl) were introduced in 4 ml glass vials. The vials were then placed at the bottom of the glass container. The glass container was then closed by a glass lid with the lead template facing downwards. The different glass vessels (containing either NH_3, Sym-triazine, Sym-triazine + NH_3, Sym-triazine + I_2, Sym-triazine + NH_3 + I_2) were placed on a hot plate at 160 °C for 1hr. After that, the glass containers were removed from the hot plate and cooled down to ambient condition for 15 min. The containers were then opened the lead halide templates untapped from the lid and dissolved in DMSO-d6 for ^{1}H liquid NMR analysis.

Characterisation methods

XRD measurements were carried out in air (RH of ~30%) using an Empyrean diffractometer (Panalytical) equipped with a PIXcel-1D detector. The diffraction patterns were measured using a Cu Kα radiation (wavelength of 1.54 Å). Secondary electron SEM images were acquired with an acceleration voltage of 3 kV using an in-lens detector in a Zeiss Gemini 2 microscope. ^{1}H liquid nuclear magnetic resonance spectrometry (NMR) was done using an AVANCE™ III HD 400 MHz Spectrometer from Bruker. The samples, the organohalide powder (≈ 20 mg) or organohalide condensates on the PbI_2/CsBr layers (2 samples of 2.5 x 2.5 cm^2 were used per condition) were dissolved in 600 µl DMSO-6d (99.8%, MagniSolv) and transferred to an NMR test tube. 1 µl of hydroiodic acid was added to acidify the solution to prevent proton exchange.[2] The thermogravimetric-mass spectrometry (TGA-MS) analysis was conducted using a Netzsch STA449F3 Jupiter differential scanning calorimetry (DSC)/TGA set-up coupled with a Netzsch QMS 403 mass spectrometer. The FAI powder sample (15 mg) was pre-ground inside an Ar-filled glovebox and loaded in an aluminium crucible sealed to prevent air and humidity exposure during the transfer to the TGA-MS system. A small hole was made in the crucible lid just before the measurement to allow sublimed species to escape. After two flushing cycles with helium gas, the samples were heated from 30 to 160 °C at 5 °C min^{-1}. The crucible was maintained at pre-selected temperatures (160 °C, 180°C, 200 °C, 220 °C and 240° C) for 30 min. Helium gas served as a carrier gas during the mass spectrometry experiment.

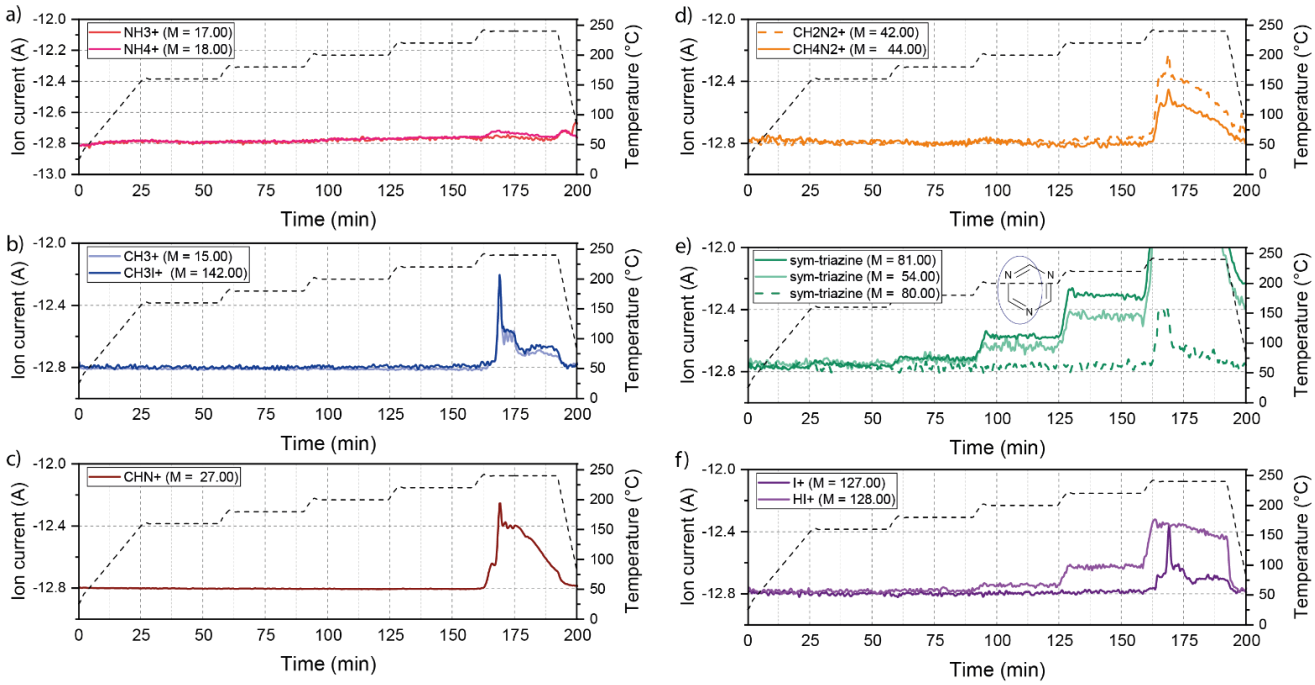

Figure S1: TGA-MS isotherms of FAI, a) ammonia (NH_3) and the ammonium cation (NH_4^+) at m/z of 17-18, b) methyl group (CH_3) and iodomethane (CH_3I) at m/z of 15 and 142, c) hydrogen cyanide (CHN) at 27 m/z, d) cyanamide (CH_2N_2) and formamidine (HCN_2H_3) at m/z of 42 and 44, e) sym-triazine fragment (HCN–(H)CN) and sym-triazine ($C_3H_3N_3$) at m/z of 54 and 81, f) iodine (I) and hydroiodic acid (HI) at m/z of 127 and 128.

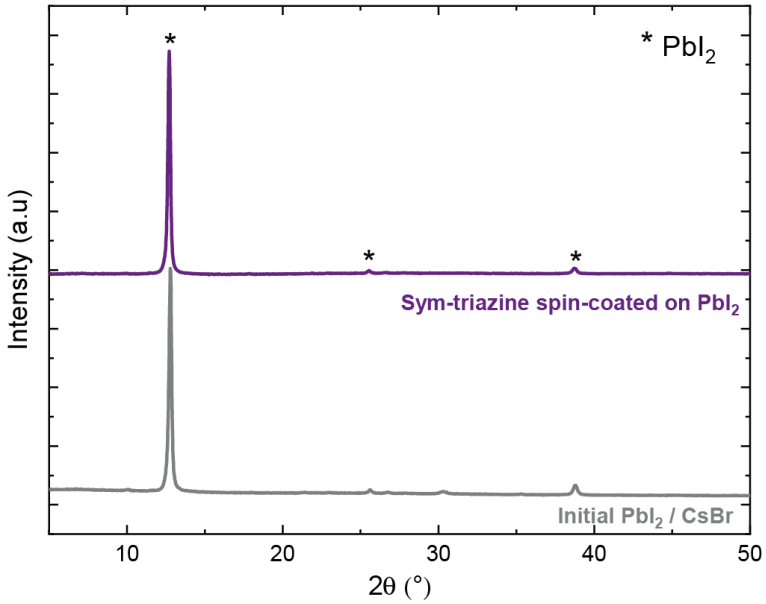

Figure S2: X-ray diffractograms of a PbI_2 layer spin-coated with sym-triazine. Spin coating a solution of sym-triazine (0.5 M) in ethanol at 3000 rpm for 30 s using dynamic solution dispensing in an inert atmosphere, followed by an annealing step (120 °C, 30 min in an N_2-filled glovebox).

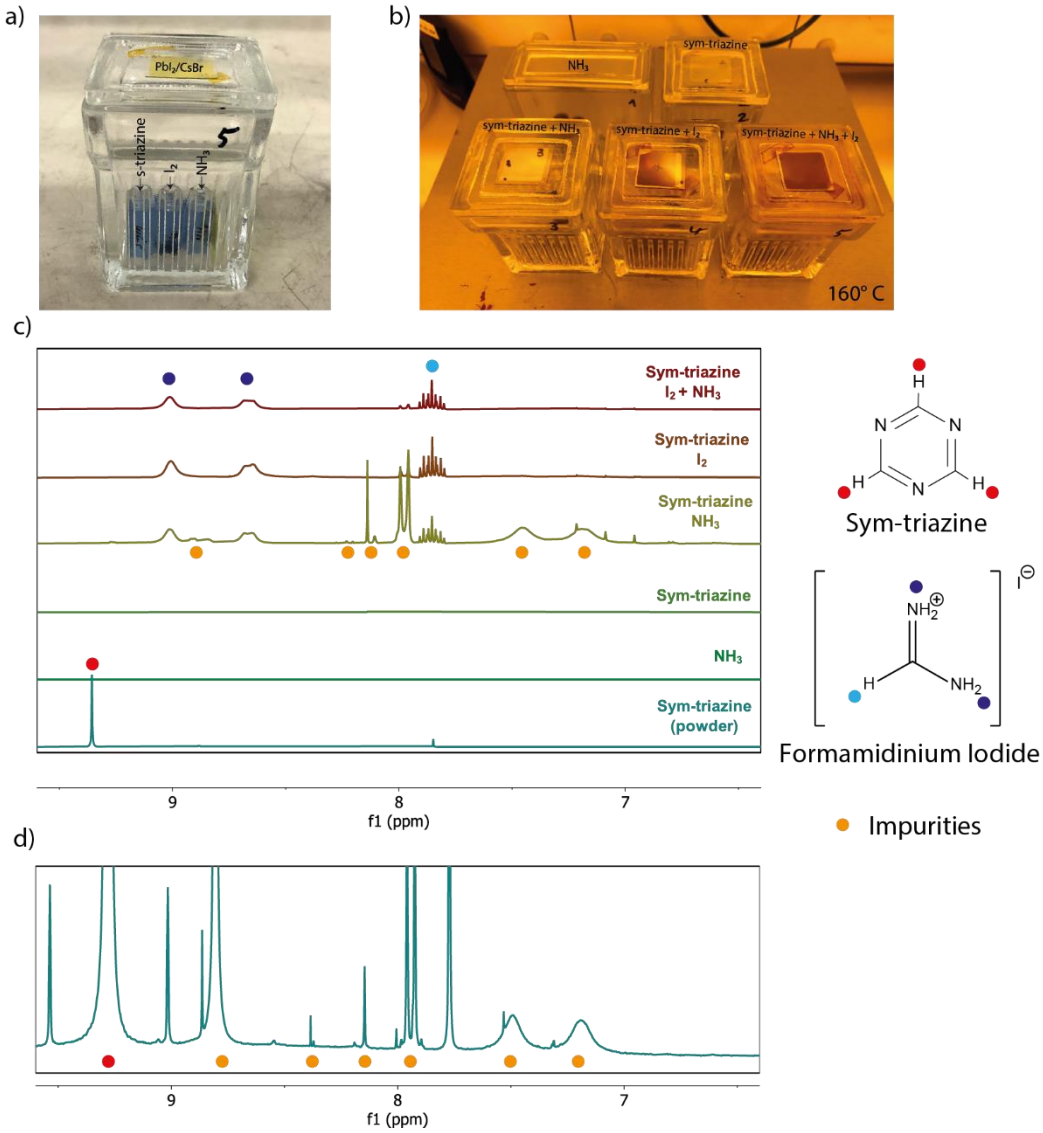

Figure S3: a) Picture of the static evaporation setup, precursors are placed in small vials, while the lead halide template is tapped to the lid of the glass container, b) picture of the experiment after 1hr at 160 °C with different precursors, c) liquid ^{1}H NMR of the condensate found on the lead halide template after the evaporation (dissolved in DMSO-d6) for the different precursor(s), d) scaled view of the liquid ^{1}H NMR of the fresh sym-triazine powder.

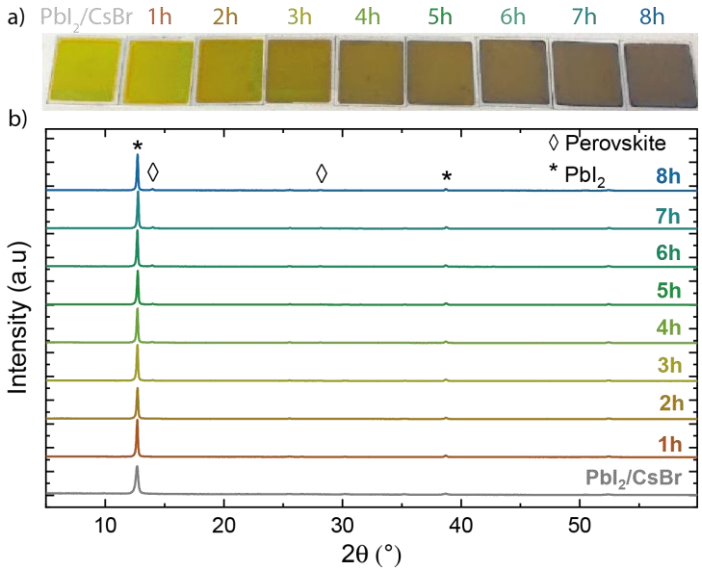

Figure S4: a) Pictures of PbI_2/CsBr layer before and after the evaporation of FAI with N_2 as carrier gas ($T_{substrate}$ = 140 °C, 1 to 8 hours of CVD evaporation), b) corresponding X-ray diffractograms.

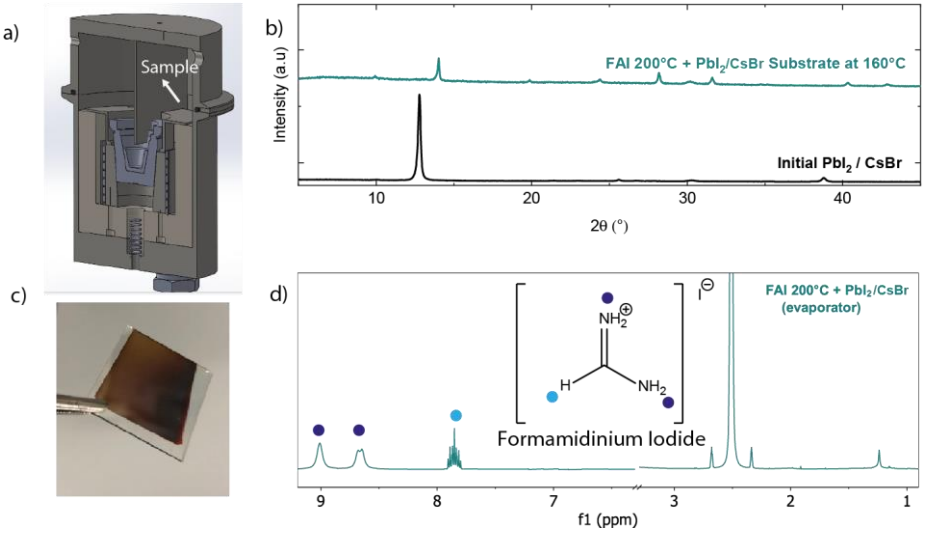

Figure S5: a) Schematic of the evaporator and the position of the PbI_2/CsBr substrate. The PbI_2/CsBr template was tapped directly on top of the evaporation unit (<10 cm from the precursor powder), b) X-ray diffractograms of the PbI_2/CsBr template before and after the evaporation of FAI, c) picture of the converted perovskite layer, d) liquid ^1H NMR of the perovskite film (dissolved in DMSO-d6).

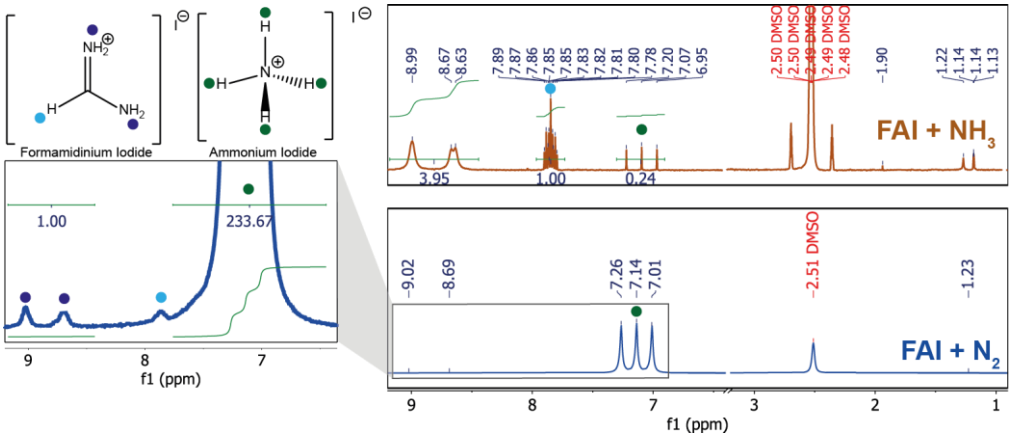

Figure S6: Liquid ^{1}H NMR of the PbI_2/CsBr layers from Figure 5 after 4 hrs of FAI evaporation with either N_2 or NH_3 as carrier gases. The left panel corresponds to a magnified view in between 6.5 and 9.2 ppm when N_2 was used as a carrier gas (the layers were dissolved in DMSO-d6).

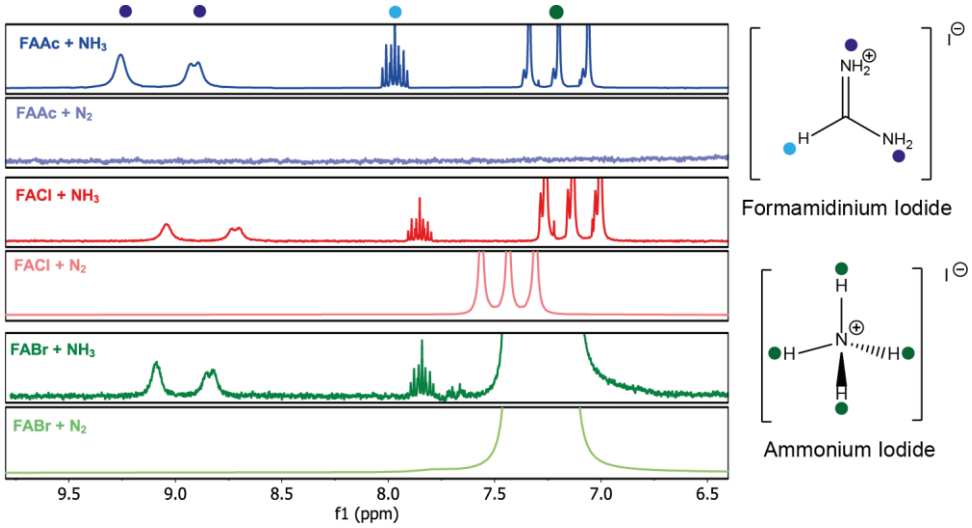

Figure S7: Liquid ^{1}H NMR of PbI_2/CsBr layers after evaporating different formamidinium salts (FABr, FACl and FAAc) with either N_2 or NH_3 as carrier gases (layers dissolved in DMSO-d6).

Notes and references

1 Sahli, F.; Miaz, N.; Salsi, N.; Bucher, C.; Schafflutzel, A.; Guesnay, Q.; Duchêne, L.; Niesen, B.; Ballif, C.; Jeangros, Q. Vapour Transport Deposition of Methylammonium Iodide for Perovskite Solar Cells. manuscrit submitted.

2 Van Gompel, W. T. M.; Herckens, R.; Reekmans, G.; Ruttens, B.; D'Haen, J.; Adriaensens, P.; Lutsen, L.; Vanderzande, D. Degradation of the Formamidinium Cation and the Quantification of the Formamidinium-Methylammonium Ratio in Lead Iodide Hybrid Perovskites by Nuclear Magnetic Resonance Spectroscopy. J. Phys. Chem. C 2018, 122 (8), 4117–4124. https://doi.org/10.1021/acs.jpcc.7b09805.